*Inorg. Chem.* **2008**, *47*, 886–895


# Synthesis and Characterization of Novel Ferrocene-Containing Pyridylamine Ligands and Their Ruthenium(II) Complexes: Electronic Communication through Hydrogen-Bonded Amide Linkage

**Takahiko Kojima,*,† Daisuke Noguchi,‡ Tomoko Nakayama,‡ Yuji Inagaki,‡,# Yoshihito Shiota,§ Kazunari Yoshizawa,§ Kei Ohkubo,† and Shunichi Fukuzumi†**

*Department of Material and Life Science, Graduate School of Engineering, Osaka University and SORST (JST), Yamada-oka, Suita, Osaka 565-0871, and Department of Chemistry, Faculty of Sciences, and Institute for Materials Chemistry and Engineering, Kyushu University, Hakozaki, Higashi-Ku, Fukuoka 812-8581, Japan*

Received August 11, 2007

Tris(2-pyridylmethyl)amine (TPA) derivatives with one or two ferrocenoylamide moieties at the 6-position of one or two pyridine rings of TPA were synthesized. The compounds, *N*-(6-ferrocenoylamide-2-pyridylmethyl)-*N*,*N*-bis(2-pyridylmethyl)amine (Fc–TPA; **L1**) and *N*,*N*-bis(6-ferrocenoylamide-2-pyridylmethyl)-*N*-(2-pyridylmethyl)amine ($Fc_2$–TPA; **L2**), were characterized by spectroscopic methods, cyclic voltammetry, and X-ray crystallography. Their Ru(II) complexes were also prepared and characterized by spectroscopic methods, cyclic voltammetry, and X-ray crystallography. [RuCl(**L1**)(DMSO)]$PF_6$ (**1**) that contains S-bound dimethyl sulfoxide (DMSO) as a ligand and an uncoordinated ferrocenoylamide moiety exhibited two redox waves at 0.23 and 0.77 V (vs ferrocene/ferrocenium ion as 0 V), due to $Fc/Fc^+$ and Ru(II)/Ru(III) redox couples, respectively. [RuCl(**L2**)]$PF_6$ (**2**) that contains both coordinated and uncoordinated amide moieties showed two redox waves that were observed at 0.27 V (two electrons) and 0.46 V (one electron), assignable to Ru(II)/Ru(III) redox couples overlapped with the uncoordinated $Fc/Fc^+$ redox couple and the coordinated $Fc/Fc^+$, respectively. In contrast to **2**, an acetonitrile complex, [Ru(**L2**)($CH_3CN$)]-($PF_6$)$_2$ (**3**), exhibited three redox couples at 0.26 and 0.37 V for two kinds of $Fc/Fc^+$ couples, and 0.83 V for the Ru(II)/Ru(III) couple (vs ferrocene/ferrocenium ion as 0 V). In this complex, the redox potentials of the coordinated and the uncoordinated Fc–amide moieties were discriminated in the range of 0.11 V. Chemical two-electron oxidation of **1** gave [$Ru^{III}$Cl(**L1**$^+$)(DMSO)]$^{3+}$ to generate a ferromagnetically coupled triplet state ($S = 1$) with $J = 13.7$ cm$^{-1}$ ($H = -JS_1S_2$) which was estimated by its variable-temperature electron spin resonance (ESR) spectra in $CH_3CN$. The electron spins at the Ru(III) center and the Fe(III) center are ferromagnetically coupled via an amide linkage. In the case of **2**, its two-electron oxidation gave the same ESR spectrum, which indicates formation of a similar triplet state. Such electronic communication may occur via the amide linkage forming the intramolecular hydrogen bonding.

## Introduction

Redox-active ligands including metallocene moieties have been developed to construct redox-responsive functional molecules[1] and molecular assemblies.[2] They have also been applied to regulation of reactivity of a Rh(I) catalyst toward different directions (hydrogenation and hydrosilylation)[3] and to control of reactivity of carbonyl ligands[4] as reported by Wrighton and co-workers. On the other hand, Mirkin and co-workers have reported on alteration of structures of metal complexes based on the redox behavior of metallocene moieties of their ligands (hemilabile ligands) to control the donicity of coordinated atoms.[5]

Among those, metallocenoylamide-containing supramolecules have been developed toward molecular recognition.

* To whom correspondence should be addressed. E-mail: kojima@chem.eng.osaka-u.ac.jp.
† Department of Material and Life Science, Osaka University and SORST (JST).
‡ Department of Chemistry, Faculty of Science, Kyushu University.
§ Institute for Materials Chemistry and Engineering, Kyushu University.
# Present address: Department of Applied Quantum Physics, Graduate School of Engineering, Kyushu University, 744 Motooka, Fukuoka 819-0395, Japan.



10.1021/ic7016038 CCC: $40.75 
Published on Web 01/09/2008

Beer, Tucker and their co-workers have reported that redox processes of the metallocene moiety could control binding constants of anionic guest molecules by changing the acidity of metallocene-connected amide N−H groups.[6] Ferrocene-containing ruthenium complexes have also been reported to exhibit not only multiple redox processes but also photoinduced intramolecular charge separation.[7] Thus, metallocenoylamide-containing ligands can be utilized to construct redox-responsive multifunctional molecular devices.

Metal complexes bearing metallocene-containing ligands have been reported to exhibit multistep redox processes and have been investigated mainly to focus on mixed-valence states of those complexes.[8,9] Dowling et al. have first reported on the observation of intervalence-transfer transitions in near-IR regions for ruthenium(II) complexes with ferrocene-containing nitrile ligands.[10] However, intramolecular magnetic interaction between the ferrocenium moiety involving a low-spin Fe(III) ($S = {}^1/_2$) and a metal ion with unpaired electron(s) has yet to be investigated. It is important to demonstrate the intramolecular magnetic interactions as a fundamental aspect of transition metal complexes with ferrocene moieties to extend their further applicability as redox-active and redox-switchable functional molecules.

We have previously reported on the synthesis, characterization, and functionality of ruthenium(II) complexes with bisamide-TPA ligands (TPA = tris(2-pyridylmethyl)amine).[11] In order to add redox-responsive property to those Ru(II) complexes, we introduced ferrocenoylamide moieties to TPA for Ru(II) complexes. In this Article, we describe the synthesis and characterization of new TPA ligands with ferrocenoylamide moiety and their Ru(II) complexes in terms of their structures and redox behavior, including formation and observation of triplet states derived from chemical oxidations of bimetallic and trimetallic Ru(II)−ferrocene systems.

## Experimental Section

**Materials and Instrumentation.** Acetonitrile ($CH_3CN$) and triethylamine ($NEt_3$) were distilled over $CaH_2$. $CH_2Cl_2$ was washed with concentrated $H_2SO_4$, followed by water, then passed through a silica gel column, and finally distilled over $CaH_2$. Methanol was refluxed and dried over Mg and then distilled prior to use. Diethyl ether was distilled from sodium benzophenone ketyl solution. All NMR measurements were performed on JEOL GX-400 and EX-270 spectrometers. UV−vis absorption spectra were measured in $CH_3CN$ on a Jasco Ubest 55 UV−vis spectrophotometer at room temperature. Infrared (IR) spectra were recorded by the Nujol method in the range of 4000−400 $cm^{-1}$ on a Jasco IR model 800 infrared spectrophotometer. Fast atom bombardment mass spectra (FAB-MS) were measured on a JMS-SX/SX102A tandem mass spectrometer. Electrospray ionization mass spectra (ESI-MS) were measured on a Perkin-Elmer Sciex API 300 mass spectrometer. All elemental analysis data were obtained at the Service Center of the Elemental Analysis of Organic Compounds, Department of Chemistry, Kyushu University.

Hydrochloric salts of *N*-(6-amino-2-pyridylmethyl)-*N*,*N*-bis(2-pyridylmethyl)amine (amino-TPA) and *N*,*N*-bis(6-amino-2-pyridylmethyl)-*N*-(2-pyridylmethyl)amine (diamino-TPA) were prepared as described previously.[11b] Ferrocenecarboxylic acid (FcCOOH), oxalyl chloride, and *N*,*N*-dimethyaminopyridine (DMAP) were purchased from Wako Pure Chemicals. $[RuCl_2(DMSO)_4]$ was synthesized in accordance with a reported procedure.[12]

**Synthesis of Chlorocarbonyl Ferrocene (FcCOCl).**[13,14] Oxalyl chloride (16.3 mL, 0.19 mol) in $CH_2Cl_2$ was added dropwise to a suspension of ferrocenecarboxylic acid (6.55 g, 28.35 mmol) in dry $CH_2Cl_2$ at 0 °C. The mixture was stirred overnight at room temperature and then was dried under reduced pressure. The residue was extracted with hexane, and the extract was dried to give FcCOCl as a red solid (6.31 g, 89% yield). IR spectrum (Nujol): $\nu_{max}/cm^{-1}$ (CO); 1765.

**Synthesis of *N*-(6-Ferrocenoylamide-2-pyridylmethyl)-*N*,*N*-bis(2-pyridylmethyl)amine (Fc−TPA; L1).** To a degassed solution containing amino-TPA (0.838 g, 2.74 mmol) and $NEt_3$ (4.2 mL, 30 mmol) in dry $CH_2Cl_2$ was added a solution of FcCOCl (0.745 g, 3 mmol) in $CH_2Cl_2$ (30 mL) dropwise, followed by the addition of DMAP (4-*N*,*N*-dimethylaminopyridine) (1.0 g, 8.2 mmol) at room temperature. The mixture was stirred for 11 h at room temperature under $N_2$. After being basified by saturated $NaHCO_3$ aqueous solution, the mixture was extracted by $CH_2Cl_2$ and the


(1) (a) Beer, P. D.; Gale, P. A.; Chen, G. Z. *Coord. Chem. Rev.* **1999**, *185*−*186*, 3−36. (b) Beer, P. D.; Gale, P. A.; Chen, G. Z. *J. Chem. Soc., Dalton Trans.* **1999**, 1897−1909. (c) Inouye, M.; Takase, M. *Angew. Chem., Int. Ed.* **2001**, *40*, 1746−1748.

(2) (a) Castro, R.; Cuadrado, I.; Alonso, B.; Casado, C. M.; Morán, M.; Kaifer, A. E. *J. Am. Chem. Soc.* **1997**, *119*, 5760−5761. (b) Astruc, D. *Acc. Chem. Res.* **2000**, *33*, 287−298.

(3) Lorkovic, I. M.; Duff, R. R., Jr.; Wrighten, M. S. *J. Am. Chem. Soc.* **1995**, *117*, 3617−3618.

(4) Lorković, I. M.; Wrighton, M. S.; Davis, W. M. *J. Am. Chem. Soc.* **1994**, *116*, 6220−6228.

(5) (a) Singlewald, E. T.; Mirkin, C. A.; Stern, C. L. *Angew. Chem., Int. Ed. Engl.* **1995**, *34*, 1624−1627. (b) Allgeier, A. M.; Stone, C. S.; Mirkin, C. A.; Liable-Sands, L. M.; Yap, G. P. A.; Rheingold, A. L. *J. Am. Chem. Soc.* **1997**, *119*, 550−559. (c) Allgeier, A. M.; Mirkin, C. A. *Angew. Chem., Int. Ed.* **1998**, *37*, 895−908. See also: (d) Miller, T. M.; Ahmed, K. J.; Wrighton, M. S. *Inorg. Chem.* **1989**, *28*, 2347−2355.

(6) (a) Szemes, F.; Hesek, D.; Chen, Z.; Dent, S. W.; Drew, M. G. B.; Goulden, A. J.; Graydon, A. R.; Grieve, A.; Mortimer, R. J.; Wear, T.; Weightman, J. S.; Beer, P. D. *Inorg. Chem.* **1996**, *35*, 5868−5879. (b) Beer, P. D. *Acc. Chem. Res.* **1998**, *31*, 71−80. (c) Carr, J. D.; Coles, S. J.; Hursthouse, M. B.; Light, M. E.; Tucker, J. H. R.; Westwood, J. *Angew. Chem., Int. Ed.* **2000**, *39*, 3296−3299. (d) Beer, P. D.; Hayes, E. J. *Coord. Chem. Rev.* **2003**, *240*, 167−189.

(7) Siemeling, U.; Von der Brüggen, J.; Vorfeld, U.; Neumann, B.; Stammler, A.; Stammeler, H.-G.; Brockhinke, A.; Plessow, R.; Zanwllo, P.; Laschi, F.; Fabrizi de Biani, F.; Fontani, M.; Steenken, S.; Stapper, M.; Gurzadyan, G. *Chem.—Eur. J.* **2003**, *9*, 2819−2833.

(8) Sixt, T.; Fiedler, J.; Kaim, W. *Inorg. Chem. Commun.* **2000**, *3*, 80−82.

(9) (a) Liu, T.-Y.; Chem, Y. J.; Tai, C.-C.; Kwan, K. S. *Inorg. Chem.* **1999**, *38*, 674−679. (b) Chen, Y. J.; Kao, C.-H.; Lin, S. L.; Tai, C.-C.; Kwan, K. S. *Inorg. Chem.* **2000**, *39*, 189−194. (c) Zhu, Y.; Clot, O.; Wolf, M. O.; Yap, G. P. A. *J. Am. Chem. Soc.* **1998**, *120*, 1812−1821. (d) Li, Z.; Beatty, A. M.; Fehler, T. P. *Inorg. Chem.* **2003**, *42*, 5707−5714. (e) Colbert, M. C. B.; Lewis, J.; Long, N. J.; Raithby, P. R.; White, A. J. P.; Williams, D. J. *J. Chem. Soc., Dalton Trans.* **1997**, 99−104.

(10) Dowling, N.; Henry, P. M.; Lewis, N. A.; Taube, H. *Inorg. Chem.* **1981**, *20*, 2345−2348.

(11) (a) Kojima, T.; Hayashi, K.; Matsuda, Y. *Chem. Lett.* **2000**, 1008−1009. (b) Kojima, T.; Hayashi, K.; Matsuda, Y. *Inorg. Chem.* **2004**, *43*, 6793−6804. (c) Kojima, T.; Miyazaki, S.; Hayashi, K.; Shimazaki, Y.; Tani, F.; Naruta, Y.; Matsuda, Y. *Chem.—Eur. J.* **2004**, *10*, 6402−6410. For others, see: (d) Jitsukawa, K.; Oka, Y.; Yamaguchi, S.; Masuda, H. *Inorg. Chem.* **2004**, *43*, 8119−8129.

(12) James, B. R.; Ochiai, E.; Rempel, G. I. *Inorg. Nucl. Chem. Lett.* **1971**, *7*, 781−784.

(13) Carr, J. D.; Coles, S. J.; Hassan, W. W.; Hursthouse, M. B.; Malik, K. M. A.; Tucker, J. H. R. *J. Chem. Soc., Dalton Trans.* **1999**, 57−62.

(14) Knobloch, F. W.; Rauscher, W. H. *J. Polym. Sci.* **1961**, *54*, 651−656.

extract was dried on anhydrous $Na_2CO_3$. After filtration, the filtrate was concentrated to a small volume and then eluted on an alumina column with ethyl acetate/hexane (2/1 v/v). A fraction ($R_f = 0.4$) was collected, and the solvents were removed under reduced pressure to give an orange powder of **L1** (0.32 g, 22% yield). Anal. Calcd for $C_{29}H_{27}N_5OFe\cdot 1/3H_2O$: C, 66.55; H, 5.33; N, 13.38. Found: C, 66.71; H, 5.41; N, 13.22. $^1$H NMR (acetone-$d_6$, $\delta$): 8.77 (br-s, 1H, N*H*), 8.38 (d, 2H, 5 Hz, py-H6), 8.02 (d, 1H, 8 Hz, py-(Fc)-H3), 7.6 (pseudo-t, 3H, py-H4 and py(Fc)-H4), 7.55 (2H, d, 8 Hz, py-H3), 7.31 (d, 1H, 8 Hz, py(Fc)-H5), 7.10 (td, 2H, py-H5, 7 and 1 Hz), 4.95 (pseudo-t, 2H, 2 Hz, H2 and H5 of substituted Cp), 4.34 (pseudo-t, 2H, 2 Hz, H3 and H4 of substituted Cp), 4.12 (Cp, 5H, s), 3.74 (s, 4H, C*H*$_2$), 3.65 (s, 2H, C*H*$_2$). IR spectrum (in KBr pellet): $\nu$/cm$^{-1}$; 1662 (C═O). Absorption maximum ($\lambda_{max}$, nm) in $CH_3CN$: 440 ($\epsilon = 865$ M$^{-1}$ cm$^{-1}$).

**Synthesis of *N*,*N*-Bis(6-ferrocenoylamide-2-pyridylmethyl)-*N*-(pyridylmethyl)amine ($Fc_2$−TPA; L2).** Diamino-TPA·3HCl was neutralized by an aqueous $NaHCO_3$ solution, extracted by $CH_2Cl_2$, and dried on $Na_2CO_3$. To a degassed solution of diamino-TPA (0.911 g, 2.84 mmol) and triethylamine (4.1 mL, 29.6 mmol) in $CH_2Cl_2$ (200 mL) was added FcCOCl (6.31 g, 25.29 mmol) in $CH_2Cl_2$ (90 mL) dropwise over a period of 30 min under $N_2$ at 0 °C. After the mixture was stirred for 1 h at 0 °C, DMAP (1.14 g, 9.32 mmol) was added, and the mixture turned red-purple. This was dried under reduced pressure after stirring for 7 h at room temperature. To the residue, a saturated $NaHCO_3$ aqueous solution (60 mL) was added, and the mixture was extracted with $CH_2Cl_2$ (3 × 100 mL). The combined extracts were dried on anhydrous $Na_2CO_3$, filtered, and the solvent was removed under reduced pressure. The crude product was purified by column chromatography on activated alumina (2:1 ethyl acetate/hexane) to give pure **L2** as an orange solid. The yield was 36% (0.753 g). Anal. Calcd for $C_{40}H_{36}N_6O_2Fe_2\cdot 2H_2O$: C, 61.55; H, 5.17; N, 10.77. Found: C, 61.36; H, 4.90; N, 10.40. FAB-MS: $m/z = 745.1$ $(M + H)^+$. $^1$H NMR ($CDCl_3$, $\delta$ (ppm)): 8.48 (d, 1H, 4.0 Hz, py-H6), 8.36 (s, 1H, NH), 8.04 (d, 2H, 8 Hz, py(Fc)-H3), 7.73 (t, 2H, 8 Hz, py-(Fc)-H4), 7.72 (t, 1H, 8 Hz, py-H4), 7.65 (d, 1H, 8 Hz, py-H3), 7.36 (d, 2H, 8 Hz, py(Fc)-H5), 7.19 (t, 1H, 6 Hz, py-H5), 4.88 (t, 4H, 2 Hz, H2 and H5 of substituted Cp), 4.45 (t, 4H, 2 Hz, H3 and H4 of substituted Cp), 4.22 (s, 10H,Cp), 3.89 (s, 2H, CH2 of py), 3.80 (s, 4H, CH2 of py(Fc)). IR spectrum (in KBr pellet): $\nu_{max}$/cm$^{-1}$ (CO); 1653. Absorption maximum ($\lambda_{max}$, nm) in $CH_3CN$: 445 ($\epsilon = 1060$ M$^{-1}$ cm$^{-1}$).

**Preparation of [RuCl(L1)(DMSO)]$PF_6$ (1).** To a solution of **L1** (100 mg, 0.193 mmol) in ethanol (20 mL), [$RuCl_2(DMSO)_4$] (97 mg, 0.200 mmol) was added in portions with vigorous stirring under $N_2$. The mixture was refluxed for 6 h, and $NH_4PF_6$ (49 mg, 0.300 mmol) was added as a solid after cooling. The solution was concentrated to a small volume (one-fifth volume) to obtain an orange powder, which was washed with ethanol and diethyl ether, then dried in vacuo (137 mg, 78% yield). Anal. Calcd for $C_{31}H_{33}N_5O_2ClSFeRuPF_6\cdot 2H_2O$: C, 40.78; H, 4.08; N, 7.67. Found: C, 40.57; H, 3.69; N, 7.83. $^1$H NMR ($CD_3CN$, $\delta$): 10.72 (br-s, 1H, N*H*), 9.60 (d, 6 Hz, 1H, ax-py-H6), 8.82 (d, 6 Hz, 1H, eq-py-H6), 8.33 (d, 8 Hz, 1H, ax-py-H3), 7.76 (t, 8 Hz, 1H, eq-py-H4), 7.75 (t, 8 Hz, 1H, eq-py(Fc)-H4), 7.68 (t, 8 Hz, 1H, ax-py-H4), 7.42 (d, 8 Hz, 1H, eq-py(Fc)-H5), 7.34 (t, 1H, 6 Hz, ax-py-H5), 7.30 (t, 1H, ex-py-H5), 7.18 (d, 1H, 8 Hz, eq-py(Fc)-H3), 7.12 (d, 1H, 7 Hz, eq-py-H3), 5.71 (AXd, 2H, 15 Hz, $CH_2$), 5.41 (pseudo-s, 1H, H5′ of Cp), 5.28 (pseudo-s, 1H, H2′ of Cp), 5.25 (AXd, 2H, 15 Hz, $CH_2$), 4.65 (AXd, 2H, 15 Hz, $CH_2$). 4.63 (AXd, 2H, 15 Hz, $CH_2$), 4.56 (pseudo-t, 2H, 2 Hz, H3 and H5 of substituted Cp), 4.51 (s, 2H, $CH_2$), 4.24 (s, 5H, Cp). IR spectrum (in KBr pellet): $\nu_{max}$/cm$^{-1}$; 1680 (C═O), 1067 (S═O). Absorption maxima ($\lambda_{max}$, nm) in $CH_3CN$: 282 ($\epsilon = 22\,800$ M$^{-1}$ cm$^{-1}$), 350 ($\epsilon = 12\,700$ M$^{-1}$ cm$^{-1}$).

**Table 1.** Crystallographic Data for **L1** and **1**

| | L1 | 1 |
|---|---|---|
| formula | $C_{29}H_{27}FeN_5O$ | $C_{31}H_{33}N_5O_2ClSFeRuPF_6$ |
| fw | 517.41 | 877.03 |
| cryst syst | monoclinic | monoclinic |
| space group | $P2_1/n$ (No. 14) | $P2_1/c$ (No. 14) |
| *A*, Å | 14.3218(10) | 12.8071(7) |
| *B*, Å | 11.1188(7) | 12.2123(5) |
| *c*, Å | 15.7468(10) | 21.5373(12) |
| $\beta$, deg | 100.953(4) | 98.431(3) |
| *V*, Å$^3$ | 2461.9(3) | 3332.1(3) |
| *Z* | 4 | 4 |
| $D_{calc}$, g/cm$^3$ | 1.396 | 1.748 |
| $\mu$(Mo K$\alpha$), cm$^{-1}$ | 6.45 | 11.52 |
| *T*, °C | −160 ± 1 | −140 ± 1 |
| no. of observns | 5545 | 7576 |
| no. of variables | 434 | 575 |
| $R^a$ | 0.052 | 0.079 |
| $Rw^b$ | 0.156 | 0.203 |
| $R1$ ($I > 2\sigma(I)$)$^c$ | 0.049 | 0.073 |
| GOF | 1.17 | 1.37 |

$^a$ $R = \sum(Fo^2 - Fc^2)/\sum Fo^2$. $^b$ $Rw = [\sum(w(Fo^2 - Fc^2)^2)/\sum w(Fo^2)^2]^{1/2}$. $^c$ $R1 = \sum||Fo| - |Fc||/\sum|Fo|$.

**Preparation of [RuCl(L2)]$PF_6$ (2).** To a degassed solution of **L2** (100 mg, 0.134 mmol) in MeOH (15 mL) was added [$RuCl_2(DMSO)_4$] (78 mg, 0.161 mmol) under $N_2$. The mixture was refluxed for 34 h and turned red during the reaction. $KPF_6$ (45 mg, 0.242 mmol) in MeOH was added to the solution under $N_2$. The mixture was concentrated under reduced pressure (one-third volume), and a red precipitate emerged. The precipitate was filtered and washed with a small volume of EtOH and $Et_2O$, and then dried. The yield was 41% (56 mg). Anal. Calcd for $C_{40}H_{36}N_6O_2Fe_2PF_6ClRu\cdot 4H_2O$: C, 43.76; H, 4.04; N, 7.65. Found: C, 43.61; H, 3.60; N, 7.42. $^1$H NMR ($CD_3CN$, $\delta$ (ppm)): 9.46 (s, 1H, NH of coordinated amide), 9.25 (s, 1H, NH of uncoordinated amide), 8.60 (d, 1H, 5 Hz, ax-py-H6), 8.44 (d, 1H, 8 Hz, py-H3), 7.76 (t, 1H, 8 Hz, py-H4), 7.62 (t, 1H, 8 Hz, py(Fc)-H4), 7.52 (t, 2H, 8 Hz, py-(Fc)-H4′), 7.05−7.17 (m, py- and py(Fc)-H3 and H5), 5.28 (AXd, 2H, 14 Hz, $CH_2$), 4.99 and 4.63 (pseudo-t, 4H, H2- and H5-Cp), 4.88 (AXd, 2H, 15 Hz, $CH_2$), 4.76 (AXd, 2H, 15 Hz, $CH_2$), 4.26 and 4.37 (pseudo-t, 4H, H3- and H4-Cp), 4.11 and 4.27 (s, 10H, Cp). FAB-MS: $m/z = 881.1$ $(M^+)$. IR spectrum (in KBr pellet): $\nu_{max}$/cm$^{-1}$ (CO); 1627 (coordinated amide), 1674 (uncoordinated amide). Absorption maxima ($\lambda_{max}$, nm) in $CH_3CN$: 345 ($\epsilon = 16\,900$ M$^{-1}$ cm$^{-1}$), 442 ($\epsilon = 12\,700$ M$^{-1}$ cm$^{-1}$).

**Preparation of [Ru(L2)($CH_3CN$)]$(PF_6)_2$ (3).** $AgNO_3$ (28 mg, 0.165 mmol) was added to a red solution of **2** (130 mg, 0.127 mmol) in $CH_3CN$ (25 mL). The mixture was refluxed for 4 h and turned orange, and AgCl emerged during the reaction. After filtration with a Celite pad, the filtrate was dried under reduced pressure. The residue was dissolved in a small volume of acetone (10 mL) and filtered. To the filtrate were added EtOH (20 mL) and $NH_4PF_6$ (40 mg, 0.245 mmol) in EtOH (20 mL), and then the solution was concentrated under reduced pressure (to $^1/_{10}$ volume) and a brown precipitate formed. The precipitate was filtered and washed with a small volume of EtOH and $Et_2O$, and then dried. The yield was 51% (76 mg). $^1$H NMR ($CD_3CN$, $\delta$ (ppm)): 9.38 (s, 1H, N*H* of coordinated Fc-amide), 9.06 (s, 1H, N*H* of free Fc-amide), 8.50 (d, 1H, 6 Hz, py-H6), 8.46 (d, 1H, 8 Hz, py-H3), 7.85 (t, 1H, 8 Hz, py-H4), 7.75 (t, 1H, 8 Hz, py(Fc)-H4), 7.67 (t, 1H, 8 Hz, py-(Fc)-H4′), 4.3−5.1 (m, Cp and $CH_2$ of pyr and substituted-py), 4.23 and 4.11 (s, 10H, Cp), 2.38 (s, 3H, $CH_3$ of $CH_3CN$). FAB-MS:

**Scheme 1.** Schematic Description for Structures of the Ligands and the Complexes Discussed in This Article[a]

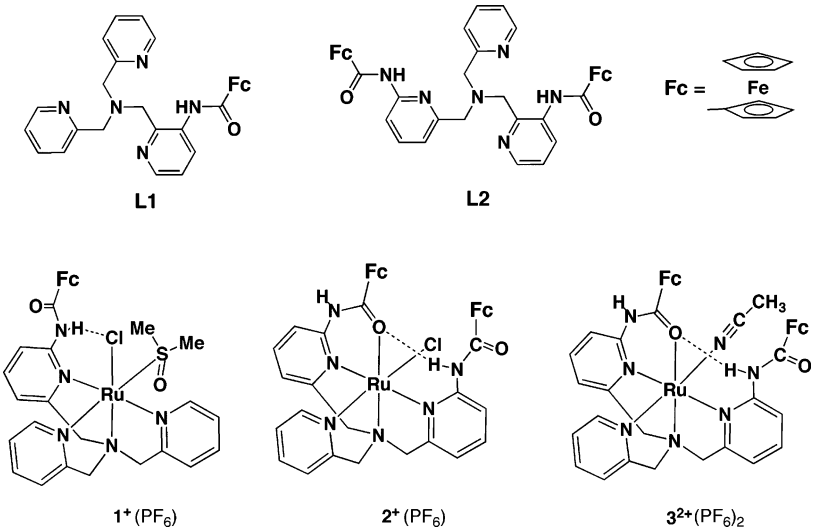


[a] Fc stands for the Fe(cyclopentadienyl)$_2$ group.

$m/z$ = 885.8 $(M - H)^+$. IR spectrum (Nujol method): $\nu_{max}/cm^{-1}$; 1626 and 1682 (CO), 2274 (C≡N). Absorption maxima ($\lambda_{max}$, nm) in $CH_3CN$: 286, 364 (sh).

**X-ray Crystallography on L1 and 1.** All measurements were made on a Rigaku Mercury CCD area detector with graphite-monochromated Mo Kα ($\lambda$ = 0.7107 Å) radiation.

A single crystal of **L1** was obtained by recrystallization from ethyl acetate. The orange platelet crystal having approximate dimensions of 0.10 × 0.10 × 0.05 mm$^3$ was mounted on a glass fiber. The data were collected at a temperature of −160 ± 1 °C to the maximum 2$\theta$ value of 55.0°. The structure was solved by direct methods and expanded using Fourier techniques. The non-hydrogen atoms were refined anisotropically. Hydrogen atoms were refined isotropically. The final cycle of full-matrix least-squares refinement on $F^2$ was based on 5455 observed reflections and 434 variable parameters. The maximum and minimum peaks on the final difference Fourier map corresponded to 0.46 and −0.47 e/Å$^3$, respectively. All calculations were performed using the CrystalStructure software package except for refinement, which was performed using SHELXL-97.[15]

A single crystal of **1** suitable for X-ray analysis was obtained by recrystallization of the crude product from MeOH. The single crystal was mounted on a glass capillary with silicon grease. The data were collected at a temperature of −140 ± 1 °C to the maximum 2$\theta$ value of 55.0°. A total of 1240 oscillation images were collected. The structure was solved by direct methods and expanded using Fourier techniques. The non-hydrogen atoms were refined anisotropically. Hydrogen atoms were refined isotropically. The final cycle of full-matrix least-squares refinement on $F^2$ was made based on 7576 observed reflections and 575 variable parameters. Neutral atom scattering factors were taken from Cromer and Waber.[16] Anomalous dispersion effects were included in $F_{calc}$; the values for $\Delta f'$ and $\Delta f''$ were those of Creagh and McAuley.[17] The values for the mass attenuation coefficients are those of Creagh and Hubbell.[18] Crystallographic data for **L1** and **1** are summarized in Table 1.

**Cyclic Voltammetry.** All cyclic voltammograms were recorded on an HECS 312B dc pulse polarograph (Fuso Electrochemical System) attached to an HECS 321B potential sweep unit of the same manufacture. Glassy carbon was employed as a working electrode. A platinum coil was used as a counter electrode, and a silver/silver nitrate ($Ag/AgNO_3$) electrode served as a reference electrode. All measurements were carried out in dry $CH_3CN$ containing 0.1 M $[(n\text{-}Bu)_4N]ClO_4$ as a supporting electrolyte under $N_2$ at ambient temperatures. The redox potentials were determined relative to the ferrocene/ferrocenium redox couple as a reference (0 V).

**Electron Spin Resonance Measurements.** Variable-temperature electron spin resonance (ESR) measurements were performed using a JEOL X-band spectrometer (JES-RE1XE) with a quartz ESR tube (1.2 mm i.d.). The solution was transferred to an ESR tube under argon. The ESR spectra of the triplet states of oxidized species of **1** and **2** were measured in frozen $CH_3CN$ at 123 K after two- or three-electron-transfer oxidation of the complexes with $[Ru(bpy)_3](PF_6)_3$ (bpy = 2,2′-bipyridine) at room temperature. The $g$ values were calibrated using a $Mn^{2+}$ marker.

ESR measurements down to 2.6 K were performed using a JEOL ES-SCKA X-band spectrometer equipped with an Oxford continuous flow cryostat (ESR910). Through the measurements, the temperature was controlled by helium flow and heater controllers (Oxford VC30 and ITC503). The magnetic field and applied frequency were monitored by a gauss meter (LakeShore450) and a microwave counter (ADVANTEST TR5212), which allowed us to determine the precise $g$ values.

**Density Functional Theory Calculations.** Density functional theory (DFT) calculations on $[Ru^{III}Cl(Fc^+\text{-}TPA)(DMSO)]^{3+}$ were carried out on a workstation. Structure optimization was made using the Los Alamos ECP with double-ζ basis for the Ru and Fe ions.[19] The D95 basis set,[20] a standard double-ζ basis, was applied for other atoms.

(15) Sheldrick, G. M. SHELX97, Programs for Crystal Structure Refinement. University of Göttingen, Germany, 1997.
(16) Cromer, D. T.; Waber, J. T. *International Tables for X-ray Crystallography*; Kynoch Press: Birmingham, England, 1974; Vol. IV, Table 2.2 A.
(17) *International Tables for X-ray Crystallography*; Kluwer Academic Publishers: Boston, MA, 1992; Vol. C.
(18) Creagh, D. C.; Hubbell, J. H. *International Tables for Crystallography*; Wilson, A. J. C., Ed.; Kluwer Academic Publishers: Boston, MA, 1992; Vol. C, Table 4.2.4.3, pp 200−206.

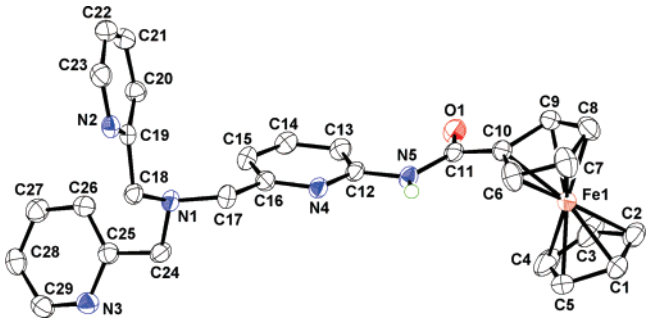


**Figure 1.** ORTEP drawing of **L1** with 50% probability thermal ellipsoids. Hydrogen atoms are omitted for clarity except that attached to the N5.

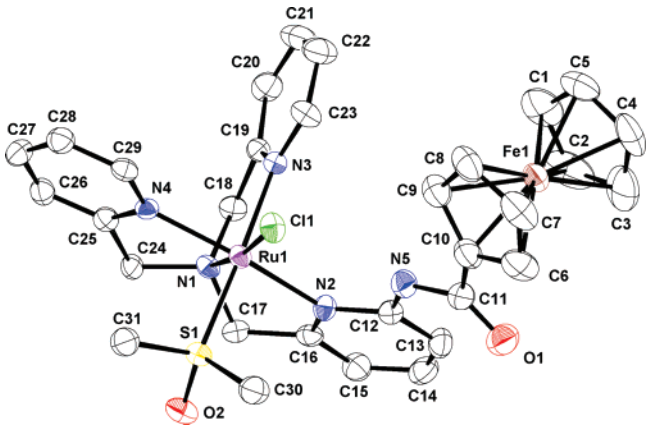


**Figure 2.** ORTEP drawing of the cationic moiety of **1** with 50% probability thermal ellipsoids. Hydrogen atoms are omitted for clarity.

## Results and Discussion

**Synthesis.** In order to synthesize **L1** and **L2**, the neutralization of the precursors, the HCl salts of amino-TPA and diamino-TPA, is indispensable prior to the amide formation with FcCOCl. Neutralized amino- and diamino-TPA should be dried using $Na_2CO_3$ after extraction with $CHCl_3$ to prepare **L1** and **L2**, respectively. When $MgSO_4$ was employed as a drying agent, no amide formation reaction occurred. In this case, the signal assigned to the H5 of ferrocene-linked pyridine showed a downfield shift, probably due to protonation by acidic $MgSO_4$ as observed in the $^1H$ NMR spectrum.

The ligands, **L1** and **L2**, were synthesized by the reactions of FcCOCl with amino-TPA and diamino-TPA in dry $CH_2Cl_2$ under $N_2$, respectively. For the synthesis of the ligands, $NEt_3$ was used as a base and DMAP was also required as an activating agent of the acid chloride to complete the reaction. In this process, it is required to add an excess mount of DMAP, probably due to both the poor nucleophilicity of the 6-amino group of the pyridine and the poor electrophilicity of the carbonyl group attached to the negatively charged cyclopentadienyl (Cp) ring. The residues treated with a saturated $NaHCO_3$ aqueous solution were extracted with $CHCl_3$. Without this process, the ligands are protonated by HCl, which is derived from the condensation of FcCOCl with the precursors, resulting in adsorption on an activated alumina.

**Table 2.** Selected Bond Lengths (angstroms) and Angles (deg) for **L1**

| | | | |
|---|---|---|---|
| Fe1−C1 | 2.039(3) | Fe1−C2 | 2.052(3) |
| Fe1−C3 | 2.041(3) | Fe1−C4 | 2.034(3) |
| Fe1−C5 | 2.031(3) | Fe1−C6 | 2.040(3) |
| Fe1−C7 | 2.046(3) | Fe1−C8 | 2.052(2) |
| Fe1−C9 | 2.049(2) | Fe1−C10 | 2.033(2) |
| O1−C11 | 1.230(2) | N5−C11 | 1.377(3) |
| N5−C12 | 1.396(3) | C10−C11 | 1.473(3) |
| O1−C11−C10 | 121.1(2) | O1−C11−N5 | 122.8(2) |
| N4−C12−N5 | 112.8(2) | | |

**Table 3.** Selected Bond Lengths (angstroms) and Angles (deg) for **1**

| | | | |
|---|---|---|---|
| Ru1−Cl1 | 2.434(1) | Ru1−S1 | 2.253(1) |
| Ru1−N1 | 2. 084(4) | Ru1−N2 | 2.131(4) |
| Ru1−N3 | 2.108(4) | Ru1−N4 | 2.078(4) |
| Fe1−Cp | 2.027 (av) | Fe1−Cp(CO) | 2.030 (av) |
| O1−C11 | 1.222(7) | N5−C11 | 1.400(7) |
| N5−C12 | 1.372(7) | C10−C11 | 1.475(8) |
| S1−O2 | 1.477(4) | | |
| S1−Ru1−Cl1 | 87.58(5) | N1−Ru1−Cl1 | 171.8(1) |
| N1−Ru1−N2 | 79.7(2) | N1−Ru1−N3 | 81.9(2) |
| N1−Ru1−N4 | 82.2(1) | N3−Ru1−S1 | 177.7(1) |
| N2−Ru1−N4 | 161.9(2) | Ru1−S1−O2 | 120.7(2) |
| N2−C12−N5 | 115.4(4) | C11−N5−C12 | 125.8(4) |
| N5−C11−O1 | 122.3(5) | N5−C11−C10 | 115.8(5) |
| O1−C11−C10 | 122.0(5) | | |

Ru(II) complexes, [RuCl(**L1**)(DMSO)]$PF_6$ (**1**) and [RuCl(**L2**)]$PF_6$ (**2**), were prepared by the reaction of [$RuCl_2$(DMSO)$_4$] with **L1** and **L2**, respectively, in MeOH by refluxing under $N_2$. The complexes should be treated under $N_2$ until $KPF_6$ is added; otherwise, the product was contaminated by unknown species. An acetonitrile complex, [Ru(**L2**)($CH_3CN$)]($PF_6$)$_2$ (**3**), was synthesized from the reaction of **1** with $AgNO_3$ in $CH_3CN$ by refluxing. The reaction to remove the chloride ligand with $Ag^+$ hardly occurred at room temperature. A schematic description of the complexes is given in Scheme 1.

**Crystal Structure of L1.** An ORTEP drawing of the compound is shown in Figure 1 with 50% probability thermal ellipsoids. Selected bond lengths are given in Table 2. The bond lengths of Fe−C(Cp) bonds are in the range of 2.031(3)−2.052(3) Å. In the crystal, an intermolecular hydrogen bond was found for N2···N5′ (3.041 Å, N2−H1′−N5′ = 160.5°). Intermolecular $\pi-\pi$ interactions were also recognized for N2···C6 (3.285 Å), C5···C14 (3.563 Å), and C4···C22 (3.618 Å) (Supporting Information). The dihedral angle between the amide plane and the Cp ring connected to the amide moiety was 7.4°, and that between the amide plane and the pyridine plane was 18.1°. This suggests that the Cp ring $\pi$-system strongly conjugates with the amide and pyridine moieties.

**Crystal Structure of 1.** A single crystal of **1** was obtained by recrystallization from MeOH. An ORTEP drawing is depicted in Figure 2 and selected bond lengths (angstroms) and angles (deg) are listed in Table 3. The Ru(II) center is surrounded by **L1** in a tetradentate fashion, chloride, and the S-bound dimethyl sulfoxide (DMSO) ligand, and the geometry is similar to that of [RuCl(1-Naph-TPA)(DMSO)]$PF_6$ (**4**) (1-Naph-TPA = *N*-(6-(1-naphthoyl)amide-2-pyridyl-

(19) (a) Dunning, T. H.; Hay, P. J. In *Modern Theoretical Chemistry*; Schaefer, H. F., III., Ed.; Plenum: New York, 1976; Vol. 3, p 1. (b) Hay, P. J.; Wadt, W. R. *J. Chem. Phys.* **1985**, *82*, 270.
(20) See ref 19b.

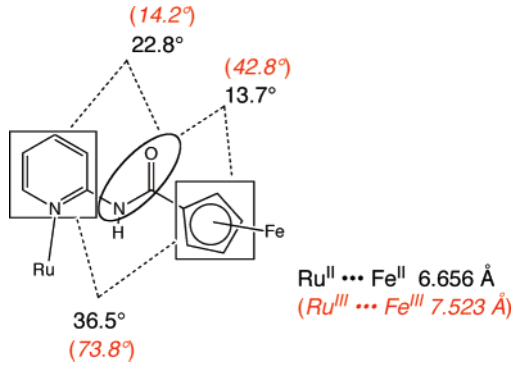


**Figure 3.** Dihedral angles of the ferrocenoylamidepyridine moiety in **1**. Values written in red are those for two-electron oxidized species of **1** obtained by DFT calculations.

methyl)-*N*,*N*-bis(2-pyridylmethyl)amine).[21] The longest Ru−N bond length was observed at Ru1−N2 (2.131(4) Å), which is involved in the ferrocenoylamide-linked pyridine. This is probably due to the spherical requirement for the intramolecular hydrogen bonding between the amide N−*H* and the chloride ligand as mentioned below. In complex **1**, the separation between the Ru(II) center and the Fe(II) center was determined to be 6.656 Å.

In complex **1**, an intramolecular hydrogen bond was found between N5 and Cl1 (3.183(4) Å) with ∠N5−H1−Cl1 = 168.6°, which was longer than that (3.135(3) Å)[21] observed in **4**. This is probably due to the reduced acidity of the N−H group in **1** arising from conjugation with negatively charged Cp ring. No significant intermolecular interaction was recognized in the crystal.

The dihedral angles around the amide moiety are described in Figure 3. The amide plane is almost coplanar with the Cp ring and the pyridine ring connected to the Fc moiety, exhibiting the dihedral angles of 13.7° and 22.8°, respectively.

**Spectroscopic Properties. A. L1 and L2.** The $^1$H NMR spectrum of **L1** was measured in acetone-$d_6$, and peak assignments were made by peak integrations and $^1$H−$^1$H COSY (correlation spectroscopy). A singlet at 3.65 ppm (2H) was assigned to the methylene protons of the ferrocenoylamide−pyridylmethyl arms, and that at 3.74 ppm (4H) was ascribed to the methylene groups for the pyridylmethyl arm. A singlet at 4.12 ppm is due to the Cp ligands of the Fc moieties, a pseudotriplet at 4.34 ppm was assigned to H3 and H4 of the substituted Cp ligands (Cp′) of the Fc moieties, and that at 4.95 ppm was assigned to H2 and H5 of the Cp′ ligands. In the range from 7 to 8.5 ppm, signals due to pyridine protons were observed and assigned as described in the Experimental Section. At 8.77 ppm, a broad singlet was detected and assigned to the amide N−*H* based on its disappearance upon addition of $D_2O$.

The IR spectrum in a KBr pellet showed a peak at 1662 cm$^{-1}$, which was assigned to amide CO vibration. The UV−vis spectrum in $CH_3CN$ showed a d−d transition band of Fe(II) in the Fc moiety at 440 nm ($\epsilon$ = 865 M$^{-1}$ cm$^{-1}$).

In the $^1$H NMR spectrum of **L2** in $CDCl_3$, a singlet at 3.80 ppm was assigned to the methylene protons for the ferrocenoylamide−pyridylmethyl arms, and that at 3.89 ppm was assigned to the methylene groups for the pyridylmethyl arm. A singlet at 4.22 ppm was assigned to the Cp ligands of the Fc moieties, a pseudotriplet at 4.45 ppm was assigned to H3 and H4 of Cp′ of the Fc moieties, and that at 4.88 ppm was assigned to H2 and H5 of the Cp′ ligands. A broad singlet at 8.36 ppm was assigned to the NH protons of the amide moieties, and the signal intensity decreased upon addition of $D_2O$. A doublet at 8.48 ppm was assigned to the H6 proton of the pyridine moiety without the ferrocenoylamide moiety.

The IR spectrum showed a peak at 1653 cm$^{-1}$, which was assigned to amide CO vibration. The UV−vis spectrum in $CH_3CN$ showed bands assigned to a $\pi-\pi^*$ transition of pyridine at 285 nm and assigned to a d−d transition of Fe(II) in the Fc moieties at 445 nm ($\epsilon$ = 1060 M$^{-1}$ cm$^{-1}$).

**B. Complex 1.** In the $^1$H NMR spectrum of **1** in $CD_3CN$, two singlets are assigned to the methyl groups of the S-bound DMSO ligand at 2.85 and 3.03 ppm. This suggests that the DMSO ligand is not allowed to rotate freely and that the two methyl groups are distinguished to be diastereotopic in a chiral coordination environment as observed in **4**.[21]

A broad singlet due to the amide hydrogen, which diminished upon addition of $D_2O$, was observed at 10.72 ppm and exhibited a large downfield shift ($\Delta\delta$ = 1.95 ppm) derived from hydrogen bonding with the chloride ligand. In the IR spectrum of **1** (in KBr pellet), a peak assigned to $\nu$(N−H) was observed at 3166 cm$^{-1}$, which was a higher value than that observed for **4** (3122 cm$^{-1}$).[21] This is consistent with the atomic distances between N(amide) and Cl$^-$ (3.183(4) Å for **1** and 3.135(3) Å for **4**),[21] indicating that the hydrogen bonding in **1** is weaker than that in **4**.

In the $^1$H NMR spectrum of **1**, signals assigned to the methylene moieties of the ligand were observed four AX doublets with a large geminal coupling constant ($J_{AX}$ = 15 Hz) at 5.71, 5.25, 4.65, and 4.63 ppm and a pseudosinglet at 4.51 ppm. This also indicates that **1** possesses a chiral environment in terms of the stereogenic tertiary amino nitrogen.[21] As for the Fc moiety, the nonsubstituted Cp ring protons exhibited a singlet at 4.24 ppm. Signals due to H2 and H5 of the Cp′ ring exhibited different chemical shifts of 5.28 and 5.41 ppm, respectively; however, they showed the same chemical shift (4.95 ppm) under noncoordinating situation. This suggests that the substituted Cp is not allowed to rotate freely because of the steric congestion by chelation of the ligand.

**C. Complex 2.** The $^1$H NMR spectrum of **2** in $CD_3CN$ showed three sets of peaks assigned to the methylene protons as follows: an AB quartet at 4.22 and 4.40 ppm ($J_{AB}$ = 12 Hz), another AB quartet at 4.57 and 4.91 ppm ($J_{AB}$ = 14 Hz), and two AX doublets at 4.64 and 5.28 ppm ($J_{AX}$ = 14 Hz).

Two sets of peaks of the ferrocene moieties were observed. Singlet peaks at 4.11 and 4.27 ppm were assigned to protons of the Cp rings of the Fc groups, which linked to the uncoordinated and the coordinated amide moieties, respectively. Two pseudotriplets at 4.26 and 4.70 ppm were assigned to resonances due to the H3 and H4 and the H2

(21) Kojima, T.; Matsuda, Y. *Chem. Lett.* **2005**, *34*, 258−259.

and H5 of the Cp′ ring of the uncoordinated Fc moiety, respectively. The other two pseudotriplets at 4.37 and 4.99 ppm were assigned to the resonances for the H3 and H4 and that of the H2 and H5 of the Cp′ of the coordinated Fc moiety, respectively. The discrimination between the two Fc moieties in **L2** also indicates that the one of amide C═O is bound to the ruthenium center to hold an asymmetric structure in $CH_3CN$. A singlet at 9.22 ppm was assigned to the NH in the uncoordinated amide, and a singlet at 9.47 ppm was assigned to the NH in the coordinated amide, based on the decrease of their peak intensities upon adding $D_2O$.

The FAB-MS spectrum of **2** showed a peak cluster assigned to $\{[RuCl(\mathbf{L2})]\}^+$ at 881.1, and its isotopic pattern agrees with the computer simulation. The IR spectrum of **2** (Nujol) showed a peak at 1622 $cm^{-1}$, assigned to CO vibration of the amide linkage, in which the oxygen binds to the Ru center, and that at 1674 $cm^{-1}$ was assigned to CO vibration for the uncoordinated counterpart, on the basis of comparison with those of uncoordinated **L1** and **L2**. Its UV−vis spectrum in $CH_3CN$ showed a band due to a $\pi-\pi^*$ transition of pyridine at 285 nm and a ligand-to-metal charge-transfer (LMCT) band from $Cl^-$ to the Ru center at 442 nm. Those values are consistent with those of structurally characterized Ru(II)−TPA complexes with two amide groups at the same positions as in **L2**.[11b]

**D. Complex 3.** The $^1H$ NMR spectrum of **3** in $CD_3CN$ showed a singlet at 2.38 ppm, which was assigned to the signal due to the C*H*$_3$ of the coordinated $CH_3CN$. Two kinds of peaks ascribed to the ferrocene moieties were also observed. A singlet at 4.11 ppm was assigned to the protons of Cp of Fc connected to the uncoordinated amide moiety. A singlet at 4.23 ppm was assigned to the protons of Cp of Fc connected to the coordinated amide linkage. These indicate that the one of the amide C═O moieties is still bound to the ruthenium center to hold the asymmetric structure as in complex **2**. A singlet at 9.06 ppm was assigned to the resonance due to the NH of the uncoordinated amide, and a broad singlet at 9.38 ppm was assigned to that of the NH of the coordinated amide, judging from their disappearance upon addition of $D_2O$.

The ESI-MS spectrum of **3** showed a peak cluster assigned to $\{[Ru(\mathbf{L2})(CH_3CN)] - H^+\}^+$ at 885.8, and its isotopic pattern was consistent with computer simulation. The UV−vis spectrum of **3** in $CH_3CN$ showed a band due to a $\pi \rightarrow \pi^*$ transition of pyridine rings at 285 nm, a metal-to-ligand charge-transfer (MLCT) band from Ru to pyridine at 371 nm. The lack of an LMCT band from $Cl^-$ to Ru at 442 nm observed for **2** to indicates that the $Cl^-$ ligand is substituted by $CH_3CN$.[22]

The IR spectrum of **3** (Nujol) showed a peak at 1626 $cm^{-1}$ assigned to the CO vibration for the coordinated amide moiety and at 1682 $cm^{-1}$ assigned to CO vibration due to the uncoordinated amide moiety, which were similar to those of **2**. In addition, a very weak peak was observed at 2274 $cm^{-1}$, assignable to $\nu$(CN) for the coordinated $CH_3CN$. This suggests that a $CH_3CN$ molecule binds to the Ru center in an $\eta^1$-N fashion. This result is consistent with other $[Ru(L)(CH_3CN)](PF_6)_2$ (L = (1-Naph)$_2$-TPA, (2-Naph)$_2$-TPA, isob$_2$-TPA, in which a $CH_3CN$ molecule is also suggested to bind to the Ru center in an $\eta^1$-N fashion.[22]

**Redox Behavior of L1, L2, and Their Ruthenium(II) Complexes.** Cyclic voltammetry (CV) of **L1**, **L2**, and their Ru(II) complexes were performed in $CH_3CN$ at room temperature in the presence of 0.1 M TBAP as an electrolyte. Redox potentials were determined relative to the ferrocene/ferrocenium ion couple as 0 V.

The cyclic voltammogram of **L1** showed one reversible redox wave at $E_{1/2} = 0.21$ V. As for **L2**, one reversible redox wave due to the $Fc/Fc^+$ couple was observed at $E_{1/2} = 0.23$ V and $\Delta E$ ($= E_{pa} - E_{pc}$) was 0.11 V at 100 mV/s. These values are comparable to that (0.24 V) of [{(6-methyl-2-pyridyl)amino}carbonyl]ferrocene reported by Carr et al.[13]

The CV of complex **1** exhibited two redox waves at 0.23 V ($\Delta E = 86$ mV) and 0.77 V ($\Delta E = 159$ mV) at the scan rate of 100 mV/s as shown in Figure 4. Based on the redox potentials of **L1**, $[RuCl(TPA)(DMSO)]^+$ (0.61 V),[23] and $[RuCl(5\text{-}Me_3\text{-}TPA)(DMSO)]^+$ (0.52 V),[23] we assigned the first redox process to the $Fc/Fc^+$ couple of the coordinated **L1** and the second one to the $Ru^{II}/Ru^{III}$ couple. The peak current for the latter process was changed in accordance with the scan rates, suggesting the second $Ru^{II}/Ru^{III}$ couple should be quasi-reversible. The higher redox potential for the $Ru^{II}/Ru^{III}$ couple results from the $\pi$-back-bonding from the ruthenium center to the S-bound DMSO ligand.[23]

Concerning the chloride complex **2**, two reversible redox couples at 0.27 and 0.46 V were observed at 20 mV/s as shown in Figure 5. The peak current of the first redox couple was twice as large as that of the following redox wave and assigned to the overlap of two redox waves due to the uncoordinated $Fc/Fc^+$ and the $Ru^{II}/Ru^{III}$ with small separation. The second redox couple at 0.46 V was assigned to the coordinated $Fc/Fc^+$ process, based on those values of $[RuCl(isob_2\text{-}TPA)]PF_6$ (0.27 V for $Ru^{II}/Ru^{III}$)[24] and **L2**. At the scan rate of 20 mV/s in the sweep range from −0.4 to 0.7 V, the reversibility of the redox couples mentioned above was intact. Therefore, no significant structural change occurs upon the one-electron oxidation of the coordinated ferrocenoylamide moieties for this complex. These results suggest that the coordination of amide oxygen is strengthened by virtue of chelation and the intramolecular hydrogen bonding and it is hard to dissociate from the Ru(II) center to maintain the structure.

In the CV of the acetonitrile complex **3** in $CH_3CN$, three redox couples were observed at 0.26 V ($\Delta E_p = 0.07$ V), 0.37 V ($\Delta E_p = 0.08$ V), and 0.83 V ($\Delta E_p = 0.14$ V) at 20 mV/s within the sweep range (from −0.25 to 1.2 V) as shown in Figure 6. In analogy with **2**, the first and second redox couples were reversible and assigned to the uncoordinated

(22) Kojima, T.; Hayashi, K.; Shiota, Y.; Tachi, Y.; Naruta, Y.; Suzuki, T.; Uezu, K.; Yoshizawa, K. *Bull. Chem. Soc. Jpn.* **2005**, *78*, 2152−2158.

(23) Kojima, T.; Amano, T.; Ishii, Y.; Ohba, M.; Okaue, Y.; Matsuda, Y. *Inorg. Chem.* **1998**, *37*, 4076−4085.

(24) See ref 11b.

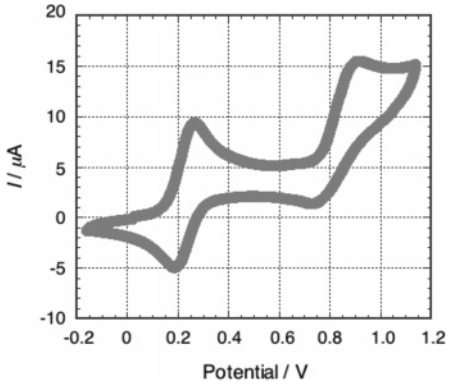


**Figure 4.** Cyclic voltammogram of **1** in $CH_3CN$ in the presence of TBAP (0.1 M) at room temperature. The potential was given relative to that of ferrocene/ferrocenium ion as 0 V.

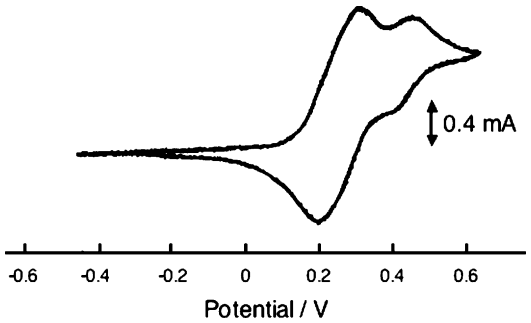


**Figure 5.** Cyclic voltammogram of **2** in $CH_3CN$ (0.1 M TBAP) at room temperature: scan rate, 20 mV/s. The potential was described relative to that of ferrocene/ferrocenium ion as 0 V.

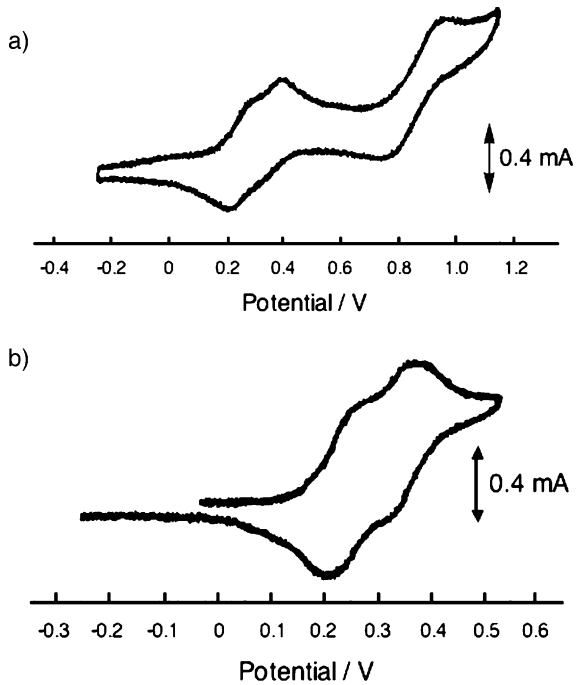


**Figure 6.** Cyclic voltammograms of $[Ru(\mathbf{L2})(CH_3CN)](PF_6)_2$ (**3**) in $CH_3CN$ (0.1 M TBAP) at room temperature: (a) scan rate, 1000 mV/s; (b) scan rate, 20 mV/s. The potential was described relative to that of ferrocene/ferrocenium ion as 0 V.

$Fc/Fc^+$ and the coordinated $Fc/Fc^+$, respectively; however, the third redox couple was irreversible on the basis of the $\Delta E_p$. In this complex, the two $Fc/Fc^+$ redox potentials can be discriminated. The coordinated Fc is directly affected by the change of the electron density at the ruthenium center. Both loss of the anionic $Cl^-$ ligand and binding of $CH_3CN$ with $\pi$-acceptor character lower the electron density at the Ru center to exert a stronger electron-withdrawing effect on the coordinated Fc moiety. This effect raises its redox potential to separate it from that of the uncoordinated counterpart. The two $Fc/Fc^+$ redox couples are intact in the change of scan rate from 20 to 1000 mV/s. This indicates that the structure is maintained upon the one-electron oxidation of the coordinated ferrocenoylamide moiety.

**Variable-Temperature ESR Measurements.** In order to clarify the oxidation processes in the Ru−Fc complexes, we examined chemical oxidations of those complexes by $[Ru(bpy)_3]^{3+}$ and measured the ESR spectra of the oxidized species in $CH_3CN$.

Two-electron oxidation of **1** ($2.0 \times 10^{-3}$ M) with two equiv of $[Ru(bpy)_3]^{3+}$ ($4.0 \times 10^{-3}$ M) in $CH_3CN$ gave $[Ru^{III}Cl(\mathbf{L1}^+)(DMSO)]^{3+}$, and its variable-temperature ESR spectrum is shown in Figure 7a. As can be seen in the spectrum, a signal assigned to that derived from a forbidden transition in a triplet state was observed at $g = 4.28$ ($\Delta m_s = 2$) and a signal due to the transition of $\Delta m_s = 1$ is at $g = 2.0038$. This spectrum is different from that of $Fc^+$, for which the $g$ values have been reported to be $g_{\parallel} = 4.36$ and $g_{\perp} = 1.30$ in acetone at 20 K.[25] The one-electron oxidation of **L1** by $[Ru(bpy)_3]^{3+}$ gave spectra exhibiting an intense signal at $g = 2.0186$ and a weak signal at $g = 4.22$ in $CH_3CN$ at 2.6 K (see the Supporting Information), which was different from that observed for the two-electron oxidized species of **1**. The peak intensity of the signal at $g = 4.28$ increased in accordance with lowering temperature down to 2.6 K, indicating that the ground state of $[Ru^{III}Cl(\mathbf{L1}^+)(DMSO)]^{3+}$ should be a triplet state ($S = 1$). The temperature-dependent change of the intensity of the signal at $g = 4.28$ ($\Delta m_s = 2$), obtained by double integration, allowed us to estimate a ferromagnetic coupling constant to be $J = 13.7$ cm$^{-1}$ ($H = -JS_1S_2$) based on curve-fitting of the data (Figure 7b) with the Bleaney−Bowers equation (Supporting Information).[26,27] This value is smaller than that ($J = 15$ cm$^{-1}$)[28] observed in a bis-$\mu$-hydroxo dinuclear Fe(II)Fe(III) complex and that ($J = 75$ cm$^{-1}$)[29] for a Cu(II)−radical complex; however, it is larger than that ($J = 1.04$ cm$^{-1}$) for an oxalato-bridged two-dimensional coordination polymer, (tetrabutylammonium)-$[Mn^{II}Ru^{III}(oxalato)_3]$.[30]

In order to gain structural insights into the triplet state, we applied DFT calculations to optimize the structure of the

(25) Prins, B.; Reinders, F. J. *J. Am. Chem. Soc.* **1969**, *91*, 4929−4931.
(26) Bleaney, B.; Bowers, K. D. *Proc. R. Soc. London, Ser. A* **1952**, *214*, 451−465. The Bleaney−Bowers equation was used to estimate the $J$ value: $IT \propto (3 + \exp(-J/kT))^{-1}$, where $H = -JS_1S_2$. The procedure for the $IT-T$ plot is described in Supporting Information.
(27) (a) Elsner, O.; Ruiz-Molina, D.; Vidal-Gancedo, J.; Rovira, C.; Veciana, J. *Chem. Commun.* **1999**, 579−580. (b) Kobayashi, K.; Ohtsu, H.; Wada, T.; Kato, T.; Tanaka, K. *J. Am. Chem. Soc.* **2003**, *125*, 6729−6739.
(28) Stubna, A.; Jo, D.-H.; Costas, M.; Brenessel, W. W.; Andres, H.; Bominaar, E. L.; Münck, E.; Que, L., Jr. *Inorg. Chem.* **2004**, *43*, 3067−3079.
(29) Luneau, D.; Rey, P. *Coord. Chem. Rev.* **2005**, *249*, 2591−2611.
(30) Larionova, J.; Mombelli, B.; Sanchiz, J.; Kahn, O. *Inorg. Chem.* **1998**, *37*, 679−684.

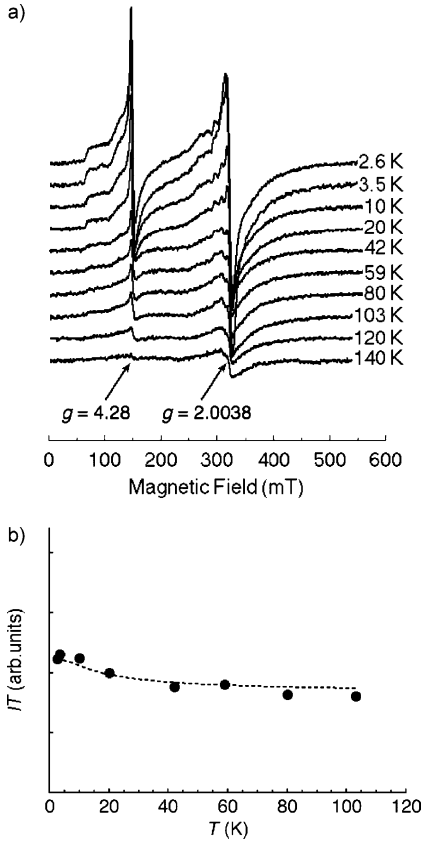


**Figure 7.** (a) Temperature-dependent ESR spectral change for the two-electron oxidized form of **1** ($2.0 \times 10^{-3}$ M) in $CH_3CN$ in the temperature range from 2.6 to 140 K. (b) Temperature dependence of *IT* of the two-electron oxidized form of **1**. The closed circles represent the experimental data, and the dotted line is the curve-fit of the data to the Bleaney−Bowers equation.

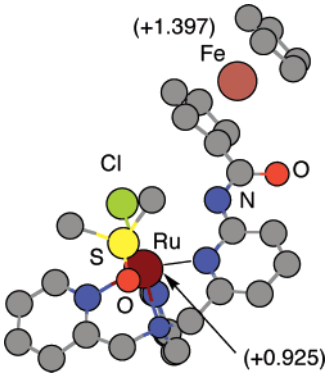


**Figure 8.** Optimized structure of the triplet state of two-electron oxidized **1**. All hydrogen atoms are omitted for clarity. Values in parentheses are the spin density at each metal center.

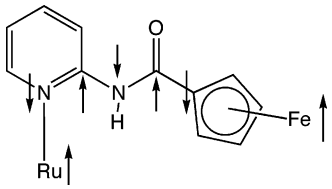


**Figure 9.** Schematic description of superexchange interaction to cause ferromagnetic coupling between Ru(III) and Fe(III) centers.

$S = 1$ state. An optimized structure is given in Figure 8. In the optimized structure, the separation between the Ru(III) center and the Fe(III) center is estimated to be 7.523 Å, which

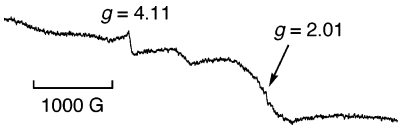


**Figure 10.** ESR spectrum of two-electron oxidized species of **2** (measured in frozen $CH_3CN$ at −150 °C): **2** ($3.3 \times 10^{-4}$ M) and $[Ru(bpy)_3](PF_6)_3$ ($6.6 \times 10^{-4}$ M).

is about 1 Å longer than that of the original singlet state (6.656 Å for the distance between Ru(II) and Fe(II) in **1**) as shown in Figure 3. The dihedral angles changed, and larger distortion was predicted between the amide plane and the Cp plane. These structural change can be derived from the electrostatic repulsion between more positively charged metal centers (Ru(III) and Fe(III)) than those in **1**. The spin density at each metal center obtained by DFT calculations is shown in Figure 8. The calculated values (+0.925 for Ru(III) and +1.397 for Fe(III)) suggest that the unpaired electrons are mainly localized at the metal centers. The magnetic interaction between Ru(III) and Fe(III) may occur through bonds rather than through space. As shown in Figure 9, the magnetization can be induced alternatively and the spins of two unpaired electrons on both metal centers can communicate to form the triplet state. The hydrogen bonding may play an important role to fix the structure of the ferrocenoylamide moiety.

We also examined the two- and three-electron oxidations of **2** with $[Ru(bpy)_3]^{3+}$ in $CH_3CN$, and ESR measurements were undertaken at −150 °C. In the case of the two-electron oxidation, the ESR spectrum of the reaction product ($[Ru^{III}Cl(\mathbf{L2}^{+})]^{3+}$) exhibited signals at $g = 2.01$ ($\Delta m_s = 1$) and $g = 4.11$ ($\Delta m_s = 2$) as shown in Figure 10. This spectrum indicates that both the ruthenium and iron centers are oxidized to form a triplet state as observed in **1**. The uncoordinated ferrocene moiety in **2** may be first oxidized as indicated by the CV (vide supra).[31]

In Scheme 2, we summarize the redox behavior of the ruthenium complexes **1**−**3**. Complex **1** exhibited two reversible redox couples; the first one at 0.23 V is due to that of the ferrocene moiety, and the second one at 0.77 V is for the ruthenium center. Complex **2** exhibited an ill-resolved two-electron redox couple for concomitant oxidation of Ru(II) center and the uncoordinated ferrocene moiety at 0.27 V, followed by the oxidation of the coordinated ferrocene part at 0.46 V. Complex **3** exhibited stepwise three redox couples for the uncoordinated Fc arm at 0.26 V followed by the coordinated Fc arm at 0.37 V and the ruthenium center at 0.83 V.

## Summary

We have synthesized and characterized novel ferrocene-containing pyridylamine ligands and their Ru(II) complexes. The two ferrocene-containing TPA ligands, **L1** and **L2**, were characterized by spectroscopic methods, electrochemical measurements, and X-ray crystallography. The crystal struc-

(31) The product of the three-electron oxidation ($[Ru^{III}Cl(\mathbf{L2}^{2+})]^{4+}$) exhibited weak ESR signals due to the residual signal of the two-electron oxidized species at −150 °C.

**Scheme 2.** Summary of Redox Behavior of **1**−**3**[a]

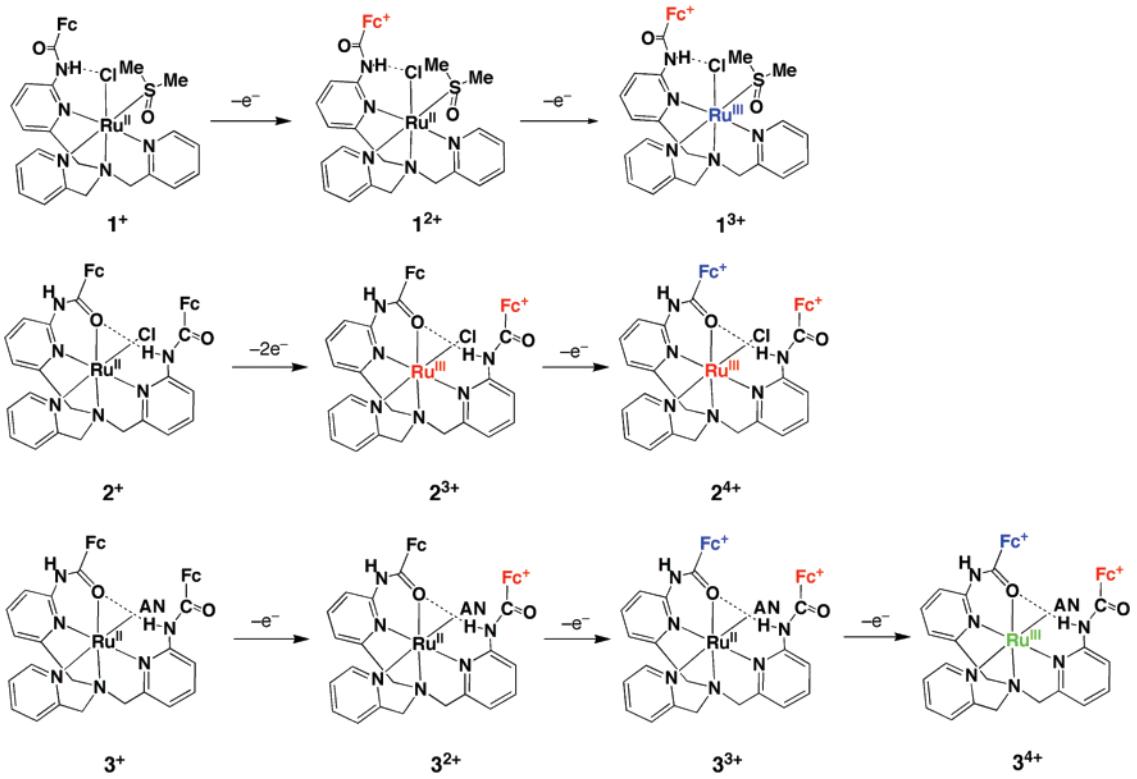


[a]AN represents the $\eta^1$-N acetonitrile ligand.

ture of the Ru(II) complex of **L1**, complex **1**, was determined to reveal that the uncoordinated ferrocenoylamide arm strongly linked to the chloride ligand via intramolecular hydrogen bonding. This complex exhibited two-step redox processes ascribed to the $Fc/Fc^+$ and Ru(II)/Ru(III) couples. The Ru(II) complexes with **L2**, **2**, and **3**, were also prepared and characterized by spectroscopic and electrochemical methods. On the basis of the spectroscopic data, those complexes have the amide-coordinating $\eta^5$-**L2** with intramolecular hydrogen bonding between the coordinated amide oxygen and the uncoordinated amide N−H group, as observed for other related bisamide-TPA complexes. The redox behavior of the complexes is revealed to show unresolved two $Fc/Fc^+$ redox couples prior to that of the Ru(II)/Ru(III) couple in the chloride complex, and the $Fc/Fc^+$ redox couples could be discriminated in the acetonitrile complex.

In the two-electron oxidation of **1** by $[Ru(bpy)_3]^{3+}$ in $CH_3CN$, the formation of the triplet ($S = 1$) species was observed. Variable-temperature ESR spectroscopy allowed us to estimate the intramolecular ferromagnetic coupling constant between $Ru^{III}$ ($S = {}^1/_2$) and $Fe^{III}$ ($S = {}^1/_2$) to be 13.7 $cm^{-1}$. As for complex **2**, two-electron oxidation took place at the Ru(II) center and the uncoordinated ferrocenoylamide moiety to give a triplet state, similar to that of **1**.

The ferrocene-containing multidentate pyridylamine ligands described here will provide new multiredox systems to exhibit the intramolecular 4d−3d ferromagnetic coupling between Ru(III) and Fe(III) centers. To our knowledge, this is the first observation of intramolecular ferromagnetic coupling in the transition metal complexes involving the ferrocenium moiety.

**Acknowledgment.** This work was supported in part by a Grant-in-Aid (No. 165500567) from The Ministry of Education, Culture, Sports, Science and Technology of Japan. We thank Professor Hiroshi Kitagawa (Kyushu University) for his kind support and helpful discussion. We appreciate Dr. Yuichi Shimazaki (Institute for Materials Chemistry and Engineering, Kyushu University) for his help in X-ray crystallography. We also thank Professor Teruo Shinmyozu (Institute for Materials Chemistry and Engineering, Kyushu University) for his kind accommodation to use their NMR spectrometer.

**Supporting Information Available:** Crystallographic data for **L1** and **1** (CIF format), crystal packing of **L1**, variable-temperature ESR of $Fc^+$-TPA in a frozen $CH_3CN$ solution, and a procedure to estimate the peak intensity of $[Ru^{III}Cl(Fc^+\text{-TPA})(DMSO)]^{3+}$. This material is available free of charge via the Internet at http://pubs.acs.org.

IC7016038